[1]Arman Irandegani

[1]*Murteza Sanjaranipour

[2]Faramarz Sarhaddi

Investigation of Thermal Stress in Annular Fins with Rectangular and Hyperbolic Profiles using Homotopy Perturbation Method

Journal of Electrical Systems

Abstract: - In this paper, using the homotopy perturbation method (HPM), the thermal stress in annular fins with rectangular and hyperbolic profiles with temperature-dependent thermal properties have been evaluated. The effect of thermal conductivity parameter, thermo-geometric parameter and thermal expansion coefficient on fin temperature distribution and its thermal stress has been investigated. The obtained results have been validated with the results of the finite difference method (FDM) and the Adomian decomposition method (ADM) of previous literatures and a good agreement was observed. By studying the obtained results, it was observed that in the fin with rectangular profile, the highest absolute value of radial stress is occurred at X=0.32, the highest value of tangential stress is occurred at X=0, and the value of zero tangential stress is obtained at X=0.3838 and in the fin with hyperbolic profile, the highest absolute value of radial stress is occurred at x=1.64, the highest value of tangential stress is occurred at x=1 and the value of zero tangential stress is obtained at x=1.6352. It was also observed that the fin with a hyperbolic profile is safer than the fin with a rectangular profile due to the lower stress level.

Keywords: Approximated analytical solution, Annular Fin, Homotopy perturbation method, Radial Stress, Tangential stress.

I. INTRODUCTION

Heat transfer is widely used in various fields of science. One of its basic applications is in the electric heat sink. Due to physical space limitations in electrical systems, it is necessary to use extended surfaces. The main purpose of using these surfaces is to increase heat transfer by increasing the side surface. As a result, the best extended surface is the one that provides the greatest heat transfer and the greatest temperature difference. These extended surfaces are called fins. It should be noted that in a suitable fin, in addition to the high heat transfer capability, which depends on its material and shape, it should also have the least amount of consumables so that its construction has the lowest cost. Therefore, an optimal mode should be found in a fin that has these conditions at the same time.

In common analyzes to investigate the thermal performance of fins, simplifying assumptions are used, including uniform temperature distribution on the fin cross-section, constant thermophysical properties, and linear boundary conditions. These assumptions transform the energy governing equation the problem from a partial differential equation (PDE) to a linear ordinary differential equation (ODE). In this situation, the corresponding ODE has an analytical solution and its solution is in terms of hyperbolic or Bessel functions. If thermophysical properties depend on temperature, ODE becomes nonlinear problem. The homotopy perturbation method can be a prime candidate for solving the nonlinear ODE governing the fins problem. This method was presented by He in 1999 [1] and expanded by He in 2000 [2]. He used this method to solve nonlinear ODE. Due to the importance and wide application of fins, many scientists in the field of physics, mathematics and especially engineering have done analytical and numerical investigation of heat transfer in fins with different profiles. Also, several researches have been conducted regarding the use of HPM to solve nonlinear differential equations, some of which will be briefly reviewed below.

In 2002, Chiu and Chen [3] calculated the thermal stresses of a circular fin with a rectangular profile using ADM. They found that the highest radial stress occurs at R=1.3 and the highest tangential stress occurs at the base of the fin. Ganji et al. [4] solved the energy equation in 2011 to find the temperature distribution in the annular fin with temperature-dependent thermal conductivity by HPM. The results of their research showed that HPM, which provides an approximate analytical solution in the form of an infinite power series, quickly converges to the solution of the problem and also has high accuracy. In 2016, Roy and Mallick [5] solved the nonlinear energy

[1]Faculty of Mathematics, University of Sistan and Baluchestan, Zahedan, Iran

[2] Department of Mechanical Engineering, University of Sistan and Baluchestan, Zahedan, Iran

* Corresponding author E-mail: sanjarani@math.usb.ac.ir

equation by HPM in a straight rectangular fin with thermal conductivity coefficient and radiation emission coefficient depending on temperature. They reported temperature distribution, fin efficiency, optimum value of dimensionless thermo-geometric parameters of fin. They also pointed out that HPM provides more suitable results than other common methods. In 2016, Mallick et al. [6] applied ADM to obtain the thermal stresses of an annular hyperbolic fin with variable heat conduction. They first obtained the temperature field of the fin using this method, then used the temperature field equation to obtain the thermal stresses. They found that the obtained results are in good agreement with the results in the literature. Roy and Ghosal in 2016 [7] used HPM to find the temperature distribution in an annular fin with temperature-dependent thermal conductivity. The results of their research showed that in the case of combined radiative-convective heat transfer, the dominant phenomenon in heat loss from the fin is convection. Also, in the case where the fin base temperature is relatively high, the phenomenon of radiant heat loss from the fin is comparable to convection. For net radiation conditions, the dimensionless parameter of the ratio of fin dimensions is a more favorable control parameter in increasing the heat transfer rate and fin efficiency compared to other parameters. In 2018, Oguntala et al. [8] used HPM to solve the governing energy equation of a heat sink with inclined porous fin and vertical porous fin. The main goal of their research was to study the thermal characteristics of the heat sink equipped with inclined porous fins. The results of their research showed that the heat sink with inclined porous fin has a higher thermal performance compared to the heat sink with vertical porous fin in the condition of equal dimensions. In 2020, Majhi and Kundu [9] obtained the temperature distribution of a circular fin disk with the help of the Frobenius series. They investigated the performance of the fin for a wide range of different geometric and thermal parameters. The results of their research showed that the maximum performance of fin for a specific value of the thermo-geometric parameter is achieved in the presence of internal heat generation. In 2020, Yontar et al. [10] used the method of complementary functions to calculate the temperature distribution, heat transfer rate, and efficiency of an annular fin made of functionally graded materials. They observed that these fins provide good thermal performance in environments with low convective heat transfer coefficient and high thermal conductivity rating parameter. In 2020, Irandegani et al. [11] used HPM to analyze the thermal performance of radiative-convective longitudinal fins with rectangular, trapezoidal, and concave parabolic profiles. The results obtained in their research showed that HPM as a powerful tool is able to solve nonlinear equations such as the energy equation of radiative-convective fins with appropriate accuracy and speed. They also found that the concave parabolic fin has the highest heat transfer rate, efficiency and effectiveness compared to two rectangular and trapezoidal fins. He and El-Dib in 2021 [12] applied HPM to solve the Duffing equation with linear damping. They compared the obtained results with the numerical solution and observed a good agreement between the results of the two methods. The solution method used in this research can be used as a template for solving various nonlinear oscillators. In 2021, He et al. [13] applied HPM to solve the fractional Toda oscillator. They compared the obtained analytical solution with the numerical solution and observed a good agreement. In 2022, Sowmya et al [14] calculated the thermal stress and temperature distribution of a ring fin with thermal properties and variable magnetic field depending on temperature using DTM-Pade. The results obtained in this research showed that increasing the heat production parameter leads to strengthening the temperature distribution, but with the increase in the magnitude of the thermo-geometric parameter and the magnetic field parameter, the thermal distribution through the fin decreases. Fallah Najafabadi et al. in 2023 [15], using Range-Kutta numerical method, the kinetic behavior and temperature distribution of a Maxwell fluid with convection from above, which is on an expanding plate in a three-dimensional environment Next, they analyzed the rotation. They also converted the governing PDEs into ODEs and solved them using HPM. They observed that the results obtained from the two methods are in good agreement. The results of their research showed that the depth of the boundary layer depends on the rotation coefficient, so as the rotation coefficient increases, the thickness of the boundary layer decreases, so the velocity of the non-Newtonian fluid decreases in all directions. In 2024, Irandegani et al. [16] used HPM to analyze the thermal performance of radiative-convective moving longitudinal fins with trapezoidal, concave and convex parabolic profiles. The results obtained in their research showed that the convex fin produces a higher dimensionless temperature of the tip of the fin compared to the trapezoidal and concave parabolic fins, the concave parabolic fin is more efficient than the two trapezoidal and convex fins and also has mass It is also less, which makes it economically viable. They also found that increasing the Peclet number increases the dimensionless temperature and efficiency of the fin.

In this paper, the effect of thermal conductivity parameter, thermo-geometric parameter and thermal expansion coefficient on temperature distribution and thermal stress of annular fin with rectangular profile and annular fin

with hyperbolic profile with temperature-dependent thermal conductivity have been calculated. At first, by writing the energy balance for the differential element of the mentioned fins, the governing equations of two problems have been obtained, then by solving these nonlinear equations, the temperature distribution function has been calculated using HPM. Finally, using the classical theory of elasticity, thermal stresses have been calculated. The obtained results are validated with the results of FDM and ADM available in the sources.

II. HOMOTOPY PERTURBATION METHOD

To explain the basic concept of the homotopy perturbation method, the following nonlinear ordinary differential equation is considered [1]:

$$A^*(u) - f(r) = 0, \quad r\epsilon\Omega \tag{1}$$

And the boundary conditions of the mentioned equation are defined as follows:

$$B^*\left(u, \frac{\partial u}{\partial X}\right) = 0, \qquad r\epsilon\Gamma \tag{2}$$

so that $A^*(u)$, B^*, $f(r)$, and r are, respectively, the differential operator, boundary operator, definite analytic function, and a member of the domain Ω. The operator $A^*(u)$ can be broken down into linear $L^*(u)$ and nonlinear $N^*(u)$ parts. Therefore, Eq. 1 can be rewritten as follows*:*

$$L^*(u) + N^*(u) - f(r) = 0. \tag{3}$$

To use the HPM, the homotopy $\theta(r,p)$: $\Omega \times [0,1] \to R$ was defined to satisfy the following relation:

$$H(\theta,p) = (1-p)[L^*(\theta) - L^*(u_0)] + p[L^*(\theta) + N^*(\theta) - f(r)] = 0. \tag{4}$$

Equation 4 can be rewritten as follows:

$$H(\theta,p) = L^*(\theta) - L^*(u_0) + pL^*(u_0) + p[N^*(\theta) - f(r)] = 0, \tag{5}$$

where $L^* = \frac{d^2}{dX^2}$, and $p\epsilon[0,1]$ is the homotopy parameter. Further, u_0 is the initial approximation of Eq. 1 that satisfies the boundary conditions stated in Eq. 2. Using on Eqs. 4 and 5, we can write*:*

$$H(\theta,0) = [L^*(\theta) - L^*(u_0)] = 0, \tag{6}$$

$$H(\theta,1) = [L^*(\theta) + N^*(\theta) - f(r)] = 0. \tag{7}$$

Therefore, when $p = 0$, the Eqs. 4 or 5 becomes a linear equation, and when $p = 1$, the original nonlinear equation is obtained. It is assumed that the solution of Eqs. 4 and 5 can be written as a power series of p in the following form:

$$\theta = \theta_0 + p\theta_1 + p^2\theta_2 + p^3\theta_3 + p^4\theta_4 + \cdots. \tag{8}$$

By substituting $p = 1$ in Eq. 8, the approximate solution of Eq. 1 is obtained as follows:

$$u = \lim_{p\to 1}\theta = \theta_0 + \theta_1 + \theta_2 + \theta_3 + \theta_4 + \cdots \tag{9}$$

Governing equations of the annular fin with rectangular profile

In Fig. 1, an axisymmetric thin annular fin with a rectangular profile made of a homogeneous isotropic material with base radius r_i, tip radius r_o and uniform thickness t is shown.

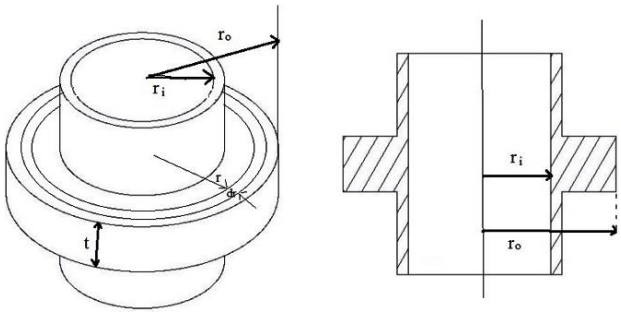

Figure 1. Annular fin with base radius r_i, tip radius r_o and thickness t.

Heat from the base of the fin enters the fin from the body at a temperature of T_b and is transferred from the side surface of the fin by convection to the environment with a temperature of T_a. The fin tip is insulated and its surface is assumed to be tension free. The thermal conductivity coefficient of the fin $(k(T))$ depends on the temperature and the convective heat transfer coefficient (h) is assumed to be constant. The temperature distribution inside the fin occurs only in the radial direction. The stress along the axis is negligible and Poisson's ratio and modulus of elasticity are assumed to be unchanged in the used temperature range. The thickness of the fin is much smaller than the radius of the fin $[t << (r_o - r_i)]$ and the heat flow in the axial direction is neglected. The axially symmetric nature of the problem (symmetric about the z axis) makes this problem independent of the tangential direction of θ. Therefore, this problem is a one-dimensional heat transfer problem along the radius r [17]. Figure 2 shows a differential element of the length of the annular fin along with the rates of different input and output energies.

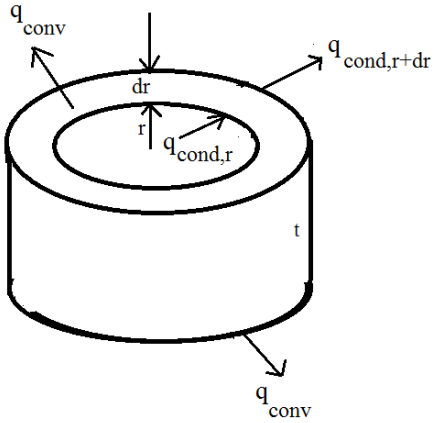

Figure 2. Differential element of the length of the annular fin.

In Fig. 2, the parameters q_{cond}, q_{conv} and t are the conduction heat transfer rate, convective heat transfer rate and fin thickness, respectively. The general form of the energy balance for a control volume is as follows:

$$\sum_{in} En - \sum_{out} En = \frac{dEn}{dt}, \tag{10}$$

where $\sum_{in} En$, $\sum_{out} En$, and $\frac{dEn}{dt}$ are, respectively, the energy rate input the control volume, the energy output rate from the control volume, and the energy change rate in the control volume. By substituting different energy components in the energy balance equation (Eq. 10) for steady-state conditions, the following relationship is obtained:

$$q_{cond,r} - q_{cond,r+dr} - 2q_{conv} = 0, \tag{11}$$

where:

$$q_{cond,r+dr} = q_{cond,r} + \frac{dq_{cond,r}}{dr} dr, \tag{12}$$

$$q_{cond,r} = -k(T)t2\pi r\frac{dT}{dr}, \tag{13}$$

$$q_{conv} = h2\pi r dr(T - T_a). \tag{14}$$

By substituting the Eqs. 12-14 in Eq. 11, the ODE governing temperature distribution over the annular fin with rectangular fin is obtained as follows [17]:

$$\frac{d}{dr}\left(k(T)tr\frac{dT}{dr}\right) = 2hr(T - T_a), \tag{15}$$

where, h is the convective heat transfer coefficient, and the heat conduction coefficient, which is a function of temperature, is defined as follows.

$$k(T) = k_a[1 + \alpha(T - T_a)], \tag{16}$$

so that the parameter k_a is the thermal conductivity at ambient temperature and the constant parameter α is the measure of the change of the thermal conductivity coefficient. For the axially symmetric case, the boundary conditions for calculating the temperature distribution are introduced as follows [17]:

$$r = r_i: \quad T = T_b, \tag{17}$$

$$r = r_o: \quad \frac{dT}{dr} = 0. \tag{18}$$

To obtain the dimensionless form of the governing equation, the dimensionless parameters have been used as follows [17]:

$$\theta = \frac{T - T_a}{T_b - T_a}, \qquad X = \frac{r - r_i}{r_i}, \qquad R = \frac{r_o}{r_i}, \qquad M = \frac{h{r_i}^2}{k_a t}, \qquad A = \alpha(T - T_a). \tag{19}$$

By applying the dimensionless parameters (Eq. 19) in the Eq. 15, the dimensionless form of the equation governing the temperature distribution of the corresponding fin is obtained as follows:

$$\frac{d^2\theta}{dX^2} + A\left(\frac{d\theta}{dX}\right)^2 + A\theta\frac{d^2\theta}{dX^2} + \frac{A}{1+X}\theta\frac{d\theta}{dX} + \frac{1}{1+X}\frac{d\theta}{dX} - 2M\theta = 0, \tag{20}$$

and also the corresponding dimensionless boundary conditions are as follows:

$$\theta(0) = 1, \tag{21}$$

$$\frac{d\theta(R-1)}{dX} = 0. \tag{22}$$

According to Eq. 20, temperature distribution is θ affected by fin radius (X), thermal conductivity (A) and thermo-geometric parameter (M).

Calculation of temperature distribution of annular fin with rectangular profile by HPM

In this part, the problem is solved with the help of HPM. Using the relation Eq.5, the Eq. 20 can be written as follows:

$$H(\theta, p) = L^*(\theta) - L^*(u_0) + pL^*(u_0) + p\left[A\left(\frac{d\theta}{dX}\right)^2 + A\theta\frac{d^2\theta}{dX^2} + \frac{A}{1+X}\frac{d\theta}{dX}\theta + \frac{1}{1+X}\frac{d\theta}{dX} - 2M\theta\right] = 0. \tag{23}$$

By substituting θ from the Eq. 8 in the Eq. 23 and by separating the different orders of p, we will have the following equations:

$$p^0: \frac{d^2\theta_0}{dX^2} - \frac{d^2u_0}{dX^2} = 0, \tag{24}$$

$$p^1: \frac{d^2\theta_1}{dX^2} + \frac{d^2u_0}{dX^2} = -A\left[\left(\frac{d\theta_0}{dX}\right)^2 + \theta_0\frac{d^2\theta_0}{dX^2} + \frac{1}{1+X}\frac{d\theta_0}{dX}\theta_0\right] - \frac{1}{1+X}\frac{d\theta_0}{dX} + 2M\theta_0, \tag{25}$$

$$p^2: \frac{d^2\theta_2}{dX^2} = -A\left[2\frac{d\theta_0}{dX}\frac{d\theta_1}{dX} + \frac{d^2\theta_1}{dX^2}\theta_0 + \frac{d^2\theta_0}{dX^2}\theta_1 + \frac{1}{1+X}\left(\frac{d\theta_1}{dX}\theta_0 + \frac{d\theta_0}{dX}\theta_1\right)\right] - \frac{1}{1+X}\frac{d\theta_1}{dX} + 2M\theta_1. \quad (26)$$

By substituting θ from Eq. 8 in the boundary conditions 21 and 22, we will have:

$$\theta(0) = \theta_0(0) + p\theta_1(0) + p^2\theta_2(0) + \cdots = 1, \quad (27)$$

by separating the different orders of p, we will have:

$$\theta_0(0) = 1, \theta_1(0) = \theta_2(0) = \cdots = 0, \quad (28)$$

we also have:

$$\frac{d\theta(R-1)}{dX} = \frac{d}{dX}[\theta_0(R-1) + p\theta_1(R-1) + p^2\theta_2(R-1) + \cdots] = 0, \quad (29)$$

by separating the different orders of p, we will have:

$$\frac{d\theta_0(R-1)}{dX} = \frac{d\theta_1(R-1)}{dX} = \frac{d\theta_2(R-1)}{dX} = \cdots = 0. \quad (30)$$

From solving the Eqs. 24-26 and using the boundary conditions (Eqs. 28 and 30) the values of θ_0, θ_1 and θ_2 will be obtained as follows:

$$\theta_0 = 1, \quad (31)$$

$$\theta_1 = MX^2 - 2M(R-1)X, \quad (32)$$

$$\theta_2 = \frac{1}{6}M\Big(X\Big(12A(R-X-2) - 6(X+2) + M\big(8R^3 + X^3 - 24R^2 + 4X^2 - 8 - 4R(X^2-6)\big)\Big) - 12RX(A+1)LnR + 12R(A+1)(X+1)Ln(1+X)\Big). \quad (33)$$

By substituting the values of θ_0, θ_1 and θ_2 in the Eq. 9, the dimensionless temperature distribution of θ is obtained as follows:

$$\theta = 1 + MX(X - 2R + 2) + \frac{1}{6}M\Big(X\Big(12A(R-X-2) - 6(X+2) + M\big(8R^3 + X^3 - 24R^2 + 4X^2 - 8 - 4R(X^2-6)\big)\Big) - 12RX(A+1)LnR + 12R(A+1)(X+1)Ln(1+X)\Big). \quad (34)$$

Calculation of thermal stresses in annular fin with rectangular profile

The annular fin with a rectangular profile is studied under a temperature gradient in the radial direction. Stresses are caused by a specific strain. Specific strain may appear as a result of phase transformation, temperature changes, etc. due to the presence of conduction-convective field. In the problem studied in the current research, temperature change in the radial direction is assumed as the only main factor in creating specific strain. Due to the fact that the thickness of the fin is much smaller compared to its radius, therefore the change of stress and displacement on the thickness has been neglected. Also, due to the axially symmetric nature of the problem, the radial and tangential stress it is independent of θ. Therefore, the present problem is an axially symmetric plane stress problem. Ignoring the volumetric force and inertial force and based on the classical theory of elasticity, the stress balance equation in the polar coordinate system is defined as follows [18]:

$$\frac{d\sigma_r}{dr} + \frac{\sigma_r - \sigma_\theta}{r} = 0, \quad (35)$$

where, the parameters σ_r and σ_θ are the radial and tangential components of the stress field, respectively. According to the classical theory of elasticity, the temperature stress-strain relationship is expressed as follows [19]:

$$\varepsilon_r = \frac{1}{E}[\sigma_r - \nu\sigma_\theta] + \gamma t, \tag{36}$$

$$\varepsilon_\theta = \frac{1}{E}[\sigma_\theta - \nu\sigma_r] + \gamma t, \tag{37}$$

where, the parameters ε_r and ε_θ are respectively the radial and tangential strain components, ν is Poisson's ratio, γ is the coefficient of thermal expansion and E is the modulus of elasticity of the fin. Eqs. 36 and 37 can be rewritten as follows:

$$\sigma_r = \frac{E}{1-\nu^2}[\varepsilon_r + \upsilon\varepsilon_\theta - (1+\upsilon)\gamma t], \tag{38}$$

$$\sigma_\theta = \frac{E}{1-\nu^2}[\varepsilon_\theta + \upsilon\varepsilon_r - (1+\upsilon)\gamma t]. \tag{39}$$

The displacement relations for the polar components of the strain in the plane strain state are as follows:

$$\varepsilon_r = \frac{du_r}{dr}, \varepsilon_\theta = \frac{u_r}{dr}. \tag{40}$$

By substituting the Eqs. 38-40 in the Eq. 35, the following differential equation is obtained:

$$\frac{d}{dr}\left(\frac{1}{r}\frac{d(ru_r)}{dr}\right) = (1+\nu)\gamma\frac{dT}{dr}. \tag{41}$$

By integrating twice from the Eq. 41, the relation related to the radial displacement is obtained as follows:

$$u_r = \frac{(1+\nu)\gamma}{r}\int_{r_i}^{r}(T-T_a)rdr + A_1 r + \frac{A_2}{r}, \tag{42}$$

where A_1 and A_2 are integration constants. The boundary condition without tension on the internal and external surfaces is as follows:

$$r = r_i, r_o: \sigma_r = 0. \tag{43}$$

Using the Eqs. 38-40, 42 and the boundary conditions 43, the integration constants of A_1 and A_1 can be obtained as follows:

$$A_1 = \frac{(1-\nu)\gamma}{{r_o}^2 - {r_i}^2}\int_{r_i}^{r_o}(T-T_a)rdr + \gamma T_a, \tag{44}$$

$$A_2 = \frac{(1+\nu)\gamma {r_i}^2}{{r_o}^2 - {r_i}^2}\int_{r_i}^{r_o}(T-T_a)rdr. \tag{45}$$

By substituting the obtained values of A_1 and A_2 in Eq. 42, the relations related to the stress field are obtained as follows:

$$\sigma_r = -\frac{\gamma E}{r^2}\int_{r_i}^{r}(T-T_a)rdr + \frac{\gamma E}{{r_o}^2 - {r_i}^2}\left(1 - \frac{{r_i}^2}{r^2}\right)\int_{r_i}^{r_o}(T-T_a)rdr, \tag{46}$$

$$\sigma_\theta = -\gamma E(T-T_a) + \frac{\gamma E}{r^2}\int_{r_i}^{r}(T-T_a)rdr + \frac{\gamma E}{{r_o}^2 - {r_i}^2}\left(1 + \frac{{r_i}^2}{r^2}\right)\int_{r_i}^{r_o}(T-T_a)rdr. \tag{47}$$

To simplify the problem, the following dimensionless parameters are considered [19]:

$$\overline{\sigma_r} = \frac{\sigma_r}{E}, \overline{\sigma_\theta} = \frac{\sigma_\theta}{E}, x = \frac{r}{r_i}, R = \frac{r_o}{r_i}, \theta = \frac{T-T_a}{T_b - T_a}, \chi = \gamma(T_b - T_a). \tag{48}$$

By substituting the dimensionless parameters (Eq. 48) in the equations of the stress field (Eqs. 46 and 47), the equations of the dimensionless stress field are obtained:

$$\overline{\sigma_r} = -\frac{\chi}{x^2}\int_1^x \theta x dx + \frac{\chi(x^2-1)}{(R^2-1)x^2}\int_1^R \theta x dx, \tag{49}$$

$$\overline{\sigma_\theta} = -\chi\theta + \frac{\chi}{x^2}\int_1^x \theta x dx + \frac{\chi(x^2+1)}{(R^2-1)x^2}\int_1^R \theta x dx. \tag{50}$$

According to the definition of x in Eq. 48 and the definition of X in Eq. 19, we can conclude that:

$$x = X + 1. \tag{51}$$

Therefore, the stress equations in terms of the dimensionless radius of X can be written as follows:

$$\overline{\sigma_r} = -\frac{\chi}{(X+1)^2}\int_0^X \theta(X+1)dX + \frac{\chi(X^2+2X)}{(R^2-1)(X+1)^2}\int_0^{R-1} \theta(X+1)dX, \tag{52}$$

$$\overline{\sigma_\theta} = -\chi\theta + \frac{\chi}{(X+1)^2}\int_0^X \theta(X+1)dX + \frac{\chi(X^2+2X+2)}{(R^2-1)(X+1)^2}\int_0^{R-1} \theta(X+1)dX. \tag{53}$$

By calculating the integrals in the Eqs. 52 and 53, the stress equations are obtained as follows:

$$\begin{aligned}\overline{\sigma_r} = {} & \frac{\chi}{180(R^2-1)(X+1)^2}(X^2 \\ & + 2X)\Big((R-1)\big(90(R+1) + M^2(R-1)^4(61R+35) - 20MR(8R^2-R-1) \\ & - 10AM(R^3+19R^2+R-9)\big) + 60(A+1)MR(3R^2-1)LnR\Big) \\ & - \frac{\chi}{(X+1)^2}\Big(\frac{1}{180}X\Big(90(X+2) \\ & + M^2X\big(-120R^2(2X+3) + 40R^3(2X+3) + 5(X+2)^2(X^2+2X-6) \\ & - 6R(4X^3+5X^2-40X-60)\big) \\ & + 10M\Big(-9AX(X+2)^2 + 2R\big(-8X^2-15X-6+A(4X^2+3X-6)\big)\Big)\Big) \\ & - \frac{1}{3}(A+1)MRX^2(2X+3)LnR + \frac{2}{3}(A+1)MR(X+1)^3Ln(X+1)),\end{aligned} \tag{52}$$

$$\begin{aligned}\overline{\sigma_\theta} = {} & \frac{\chi}{180(R^2-1)(X+1)^2}(X^2+2X \\ & + 2)\Big((R-1)\big(90(R+1) + M^2(R-1)^4(61R+35) - 20MR(8R^2-R-1) \\ & - 10AM(R^3+19R^2+R-9)\big) + 60(A+1)MR(3R^2-1)LnR\Big) \\ & + \frac{\chi}{(X+1)^2}\Big(\frac{1}{180}X\Big(90(X+2) \\ & + M^2X\big(-120R^2(2X+3) + 40R^3(2X+3) + 5(X+2)^2(X^2+2X-6) \\ & - 6R(4X^3+5X^2-40X-60)\big) \\ & + 10M\Big(-9AX(X+2)^2 + 2R\big(-8X^2-15X-6+A(4X^2+3X-6)\big)\Big)\Big) \\ & - \frac{1}{3}(A+1)MRX^2(2X+3)LnR + \frac{2}{3}(A+1)MR(X+1)^3Ln(X+1)\Big) - \chi(1 \\ & + MX(X-2R+2) \\ & + \frac{1}{6}M\Big(X\Big(12A(R-X-2) - 6(x+2) \\ & + M\big(X^3+4X^2+8R^3-24R^2-8-4R(X^2-6)\big)\Big) - 12(A+1)RXLnR \\ & + 12(A+1)(X+1)RLn(X+1)\Big).\end{aligned} \tag{53}$$

Results of calculating the thermal stress of the annular fin with rectangular profile

The main goal in this section is to find the dimensionless temperature distribution and thermal stresses in an annular fin with a rectangular profile using HPM. First, HPM has been used to find the dimensionless temperature

distribution of the annular fin with a rectangular profile with variable thermal conductivity, and then the approximate analytical solution of the temperature distribution has been used to calculate the thermal stresses. For validation, the temperature distribution results obtained in the present problem using HPM, with the results obtained by Arslan Turk [17] using FDM, ADM and the exact answer for The dimensionless parameters M=0.3 and R=2 are compared in the Table 1. According to Table 1, it can be seen that for the thermal conductivity $A = 0.3$, the results obtained from HPM have a slightly higher temperature distribution than the results obtained from FDM, and also the results obtained from HPM has a lower temperature distribution than the results obtained from ADM. For constant thermal conductivity (A=0), the results of HPM are slightly lower than the exact results. By examining the data, it can be seen that the maximum error of HPM results compared to the results obtained from FDM, ADM and the exact results are 2.03%, 1.2% and 0.9% respectively. Therefore, it can be said that the results of HPM are in good agreement with the results obtained from FDM, ADM and the exact results.

Table 1. Comparing the dimensionless temperature distribution obtained by HPM with results of reference of [17].

	$A = 0.3$			$A = 0$	
X	FDM [17]	ADM [17]	HPM	Exact [17]	HPM
0	1	1	1	1	1
0.1	0.9477	0.9512	0.9455	0.9355	0.9345
0.2	0.9036	0.9102	0.9013	0.8820	0.8797
0.3	0.8668	0.8761	0.8659	0.8379	0.8342
0.4	0.8365	0.8481	0.8380	0.8018	0.7971
0.5	0.8119	0.8256	0.8165	0.7730	0.7673
0.6	0.7927	0.8080	0.8005	0.7504	0.7443
0.7	0.7782	0.7950	0.7891	0.7336	0.7272
0.8	0.7682	0.7862	0.7816	0.7221	0.7156
0.9	0.7624	0.7811	0.7775	0.7154	0.7089
1	0.7605	0.7795	0.7763	0.7132	0.7067

In order to validate the results of the radial and tangential stresses of the current research obtained by HPM with the results obtained by Chiu and Chen [3] with the help of ADM in Table 2 has been compared. For this purpose, the following values are considered:

$$h = 50\frac{W}{m^2K}, k_a = 186\frac{W}{mK}, t = 0.004m, \alpha = 0.00018. \quad (54)$$

By checking the data in the Table 2, it can be seen that the results related to the dimensionless temperature and thermal stresses obtained in the present problem are in good agreement with the results in the reference [3].

Table 2. Comparison of thermal stresses obtained by HPM with results of reference of [3].

	θ	θ	$\overline{\sigma_r}$	$\overline{\sigma_r}$	$\overline{\sigma_\theta}$	$\overline{\sigma_\theta}$
$\frac{r}{r_i} = X + 1$	ADM [3]	HPM	ADM [3]	HPM	ADM [3]	HPM
1	2	2	0	0	-29.7	-30.92
1.5	1.936	1.933	-5.24	-5.42	-5.51	-5.64
2	1.899	1.894	-3.89	-3.99	4.52	4.73
2.5	1.878	1.874	-1.78	-1.78	8.21	8.63
3	1.869	1.868	0	0	8.56	8.67

Figure 3 shows the effect of parameter A on the dimensionless temperature distribution, which is a function of the radius of the fin (X). As seen in this figure, the temperature gradually decreases from the base to the tip of the fin for different values of $A = -0.1, 0$, and 0.1. Also, the dimensionless temperature increases with the increase of A.

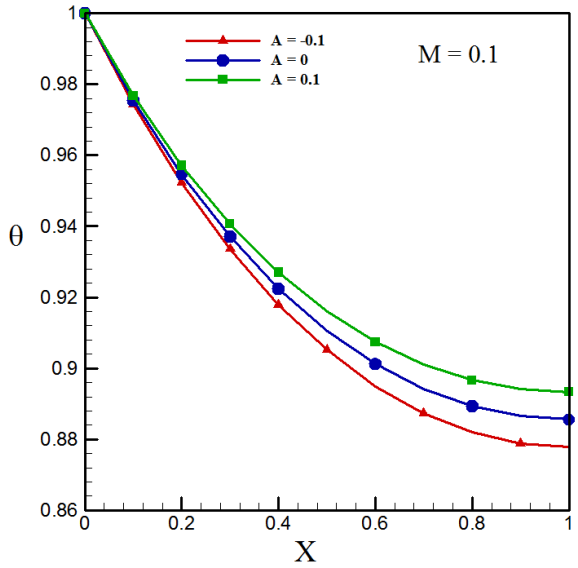

Figure 3. Effect of A on dimensionless temperature distribution.

In Figure 4, the temperature distribution changes for different values of M are shown. As can be seen, the temperature from the base to the tip of the fin decreases for different values of $M = 0.1, 0.2, 0.3$ and with the increase of M, the local temperature drop is greater.

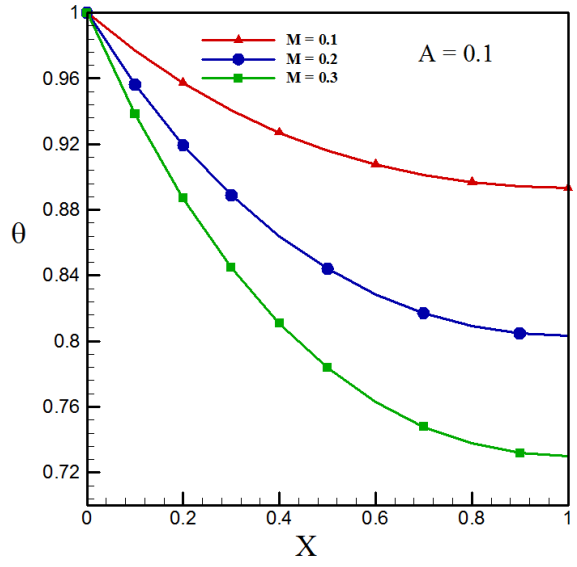

Figure 4. Effect of M on dimensionless temperature distribution.

Due to the fact that in the design process of fins, it is necessary to have appropriate information regarding temperature distribution and thermal stresses, so in this part of the research, the thermal stresses of fins have been studied. In Figures 5 and 6, the effect of thermal conductivity parameter (A) on radial stress $(\overline{\sigma_r})$ and tangential stress $(\overline{\sigma_\theta})$ is shown for values of $M = 0.1$ and $\chi = 1$. By examining these figures, the radial stresses appear to be compressive while the tangential stresses are compressive near the base and tensile near the tip of the fin. It can also be seen that the absolute value of the stress increases with the decrease of the A.

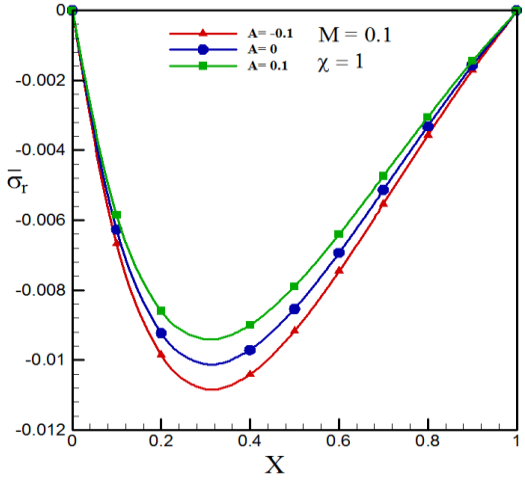

Figure 5. Effect of A parameter on radial stress.

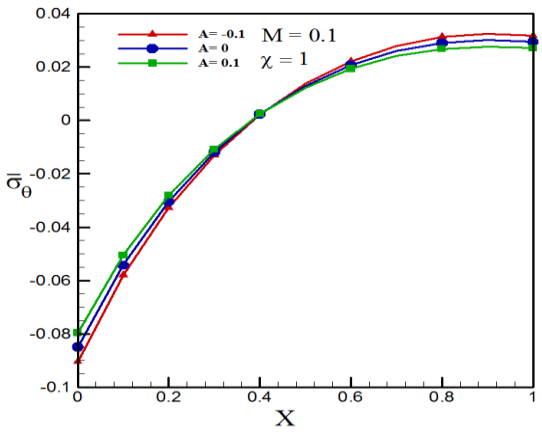

Figure 6. Effect of parameter A on tangential stress.

Figures 7 and 8 show the behavior of thermal stresses for different values of M parameter. Examining these figures similar to the previous case, the radial stresses appear to be compressive while the tangential stresses are compressive near the base and tensile near the free tip of the fin. It can also be seen that with the increase of the parameter M, the absolute value of the stress increases and the effect of the parameter M on the stress is more obvious compared to the parameter A.

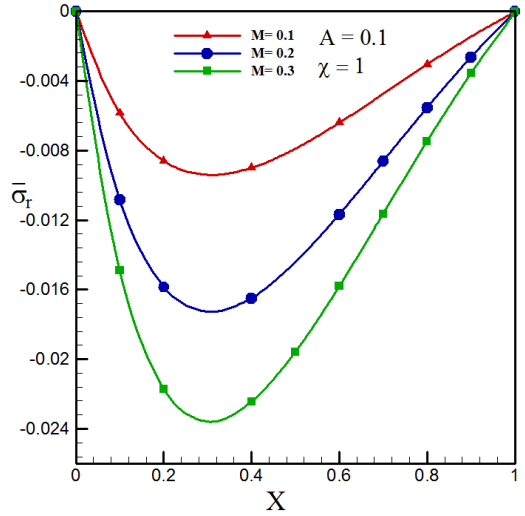

Figure 7. Effect of parameter M on radial stress.

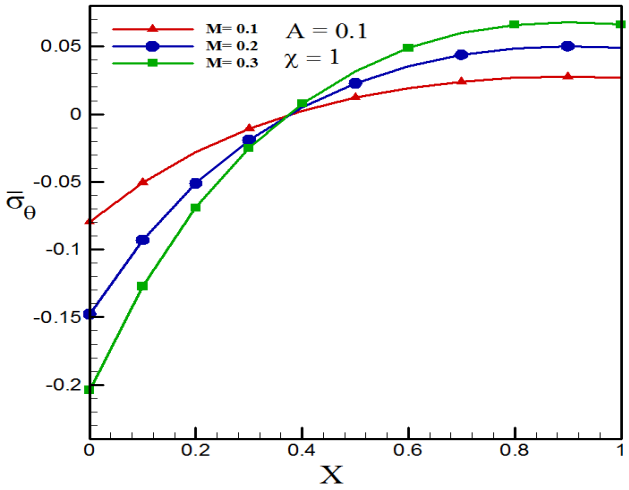

Figure 8. Effect of parameter M on tangential stress.

Figures 9 and 10 show the effect of thermal expansion parameter (χ) on radial and tangential stresses. The stress curves in the radial and tangential directions show that the radial and tangential stresses have a strong dependence on χ. It can also be seen that the absolute value of the stress increases with the increase of the χ.

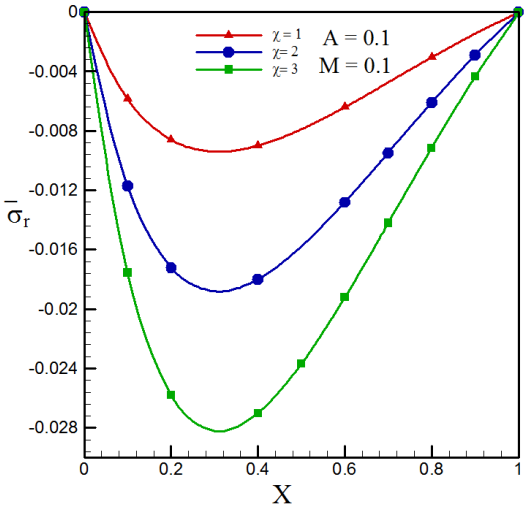

Figure 9. Effect of parameter χ on radial stress.

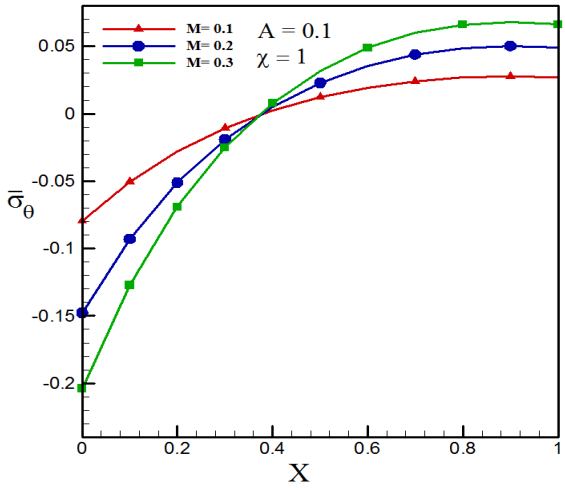

Figure 10. Effect of parameter χ on tangential stress.

By examining the Figures 3-10, it was observed that the thermal stresses are influenced by the parameters A, M and χ, while the distribution temperature is only affected by A and M. The highest absolute value of radial stress occurs at $X = 0.32$, the highest absolute value of tangential stress occurs at $X = 0$, and zero tangential stress value occurs at $X = 0.3838$. It is also observed that the maximum value of tangential stress is higher than the maximum value of radial stress. Therefore, the most effective stress on the failure of the fin, which is at the base of the fin, is the tangential stress.

Governing equations of the annular fin with hyperbolic profile

In this section, an axisymmetric annular fin with a hyperbolic profile (Fig. 11) is considered. This fin has base radius r_a and tip radius r_b and variable thermal conductivity coefficient $(k(T))$.

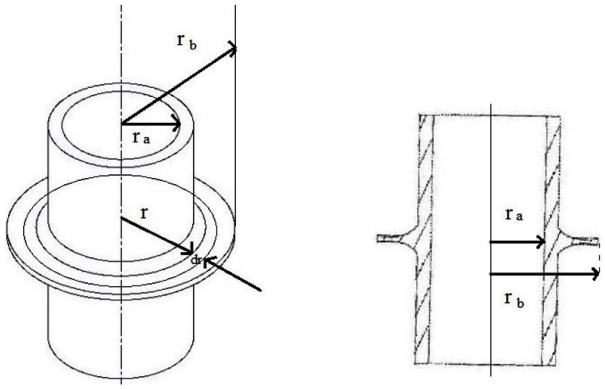

Figure 11. Annular fin with hyperbolic profile (base radius r_a, tip radius r_b).

The fin profile function is defined as follows:

$$t = \delta \left(\frac{r}{r_a}\right)^n, \tag{55}$$

where n is the profile parameter. If the value of $n = -1$ is substituted in the mentioned relationship, the fin will be hyperbolic. Heat from the base of the fin enters the fin from the body at a temperature of T_b and is transferred from the side surface of the fin by convection to the environment with a temperature of T_a. The fin tip is insulated and its surface is assumed to be tension free. The thermal conductivity coefficient of the fin $(k(T))$ depends on the temperature and the thickness of the fin is small compared to its radius. The distribution of temperature and stress is only assumed in the radial direction [6]. The differential element of the length of the annular fin along with the input and output energy rates is shown in the figure 12.

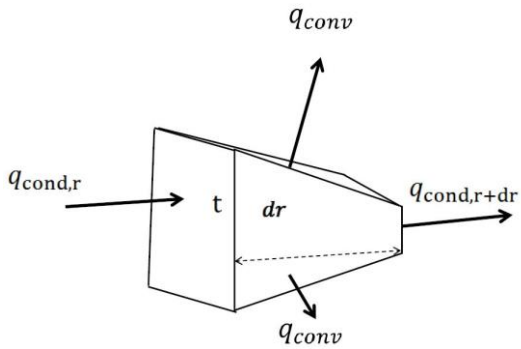

Figure 12. Differential element of the length of the annular fin with hyperbolic profile.

In Fig. 12, the parameters q_{cond}, q_{conv} and t are the conduction heat transfer rate, convective heat transfer rate and fin thickness, respectively. The general form of the energy balance for a control volume is as follows:

$$\sum_{in} En - \sum_{out} En = \frac{dEn}{dt}, \tag{56}$$

where $\sum_{in} En$, $\sum_{out} En$, and $\frac{dEn}{dt}$ are, respectively, the energy rate input the control valume, the energy output rate from the control volume, and the energy change rate in the control volume. By substituting different energy components in the energy balance equation (Eq. 56), we will have the following relationship for steady-state conditions:

$$q_{cond,r} - q_{cond,r+dr} - 2q_{conv} = 0, \tag{57}$$

where:

$$q_{cond,r+dr} = q_{cond,r} + \frac{dq_{cond,r}}{dr} dr, \tag{58}$$

$$q_{cond,r} = -k(T)t2\pi r \frac{dT}{dr}, \tag{59}$$

$$q_{conv} = h2\pi r dr(T - T_a). \tag{60}$$

By substituting the Eqs. 58-60 in Eq. 57 and by simplifying the relations, the governing equation for fin temperature distribution is obtained as follows [20]:

$$\frac{d}{dr}\left(k(T)tr\frac{dT}{dr}\right) = 2hr(T - T_a), \tag{61}$$

where, h is the convective heat transfer coefficient, and the heat conduction coefficient, which is a function of temperature, is defined as follows:

$$k(T) = k_a[1 + \alpha(T - T_a)], \tag{62}$$

so that the parameter k_a is the thermal conductivity at ambient temperature and the constant parameter α is the measure of the change of the thermal conductivity coefficient. To obtain the dimensionless form of the governing equation, the dimensionless parameters are defined as follows [6]:

$$\theta = \frac{T - T_a}{T_b - T_a}, \qquad X = \frac{r - r_a}{r_a}, \qquad R = \frac{r_b}{r_a}, \qquad \psi = \sqrt{\frac{2hr_a{}^2}{k_a\delta}}, \qquad A = \alpha(T - T_a). \tag{63}$$

By substituting the dimensionless relations (Eq. 63) in the Eq. 61, the dimensionless form of the equation governing the temperature distribution of the corresponding fin is obtained as follows:

$$\frac{d^2\theta}{dX^2} + A\left(\frac{d\theta}{dX}\right)^2 + A\theta\frac{d^2\theta}{dX^2} - \psi^2(X + 1)\theta = 0, \tag{64}$$

and also the corresponding dimensionless boundary conditions are as follows:

$$\theta(0) = 1, \tag{65}$$

$$\frac{d\theta(R - 1)}{dX} = 0. \tag{66}$$

According to Eq. 64, temperature distribution is θ affected by fin radius (X), thermal conductivity (A) and thermo-geometric parameter (ψ).

Calculation of Temperature Distribution of Annular Fin with Hyperbolic Profile by HPM

In this part, the solution of the governing equation (Eq. 64) is discussed with the help of HPM. Using the Eq. 5, the Eq. 64 can be written as follows:

$$H(\theta, p) = L^*(\theta) - L^*(u_0) + pL^*(u_0) + p\left[A\left(\frac{d\theta}{dX}\right)^2 + A\theta\frac{d^2\theta}{dX^2} - \psi^2(X + 1)\theta\right] = 0. \tag{67}$$

By substituting θ from the Eq. 8 in the Eq. 67 and by separating the different orders of p, we will have the following equations:

$$p^0: \frac{d^2\theta_0}{dX^2} - \frac{d^2u_0}{dX^2} = 0, \tag{68}$$

$$p^1: \frac{d^2\theta_1}{dX^2} + \frac{d^2u_0}{dX^2} = -A\left[\left(\frac{d\theta_0}{dX}\right)^2 + \theta_0\frac{d^2\theta_0}{dX^2}\right] + \psi^2(X+1)\theta_0, \tag{69}$$

$$p^2: \frac{d^2\theta_2}{dX^2} = -A\left[2\frac{d\theta_0}{dX}\frac{d\theta_1}{dX} + \frac{d^2\theta_1}{dX^2}\theta_0 + \frac{d^2\theta_0}{dX^2}\theta_1\right] + \psi^2(X+1)\theta_1. \tag{70}$$

By substituting θ from Eq. 8 in the boundary conditions 65 and 66, we will finally have:

$$\theta_0(0) = 1, \theta_1(0) = \theta_2(0) = \cdots = 0, \tag{71}$$

$$\frac{d\theta_0(R-1)}{dX} = \frac{d\theta_1(R-1)}{dX} = \frac{d\theta_2(R-1)}{dX} = \cdots = 0. \tag{72}$$

From solving the Eqs. 68-70 and using the boundary conditions 71 and 72 the values of θ_0, θ_1 and θ_2 will be obtained as follows:

$$\theta_0 = 1, \tag{73}$$

$$\theta_1 = \tfrac{1}{6}\psi^2X(X^2 - 3R^2 + 3X + 3), \tag{74}$$

$$\theta_2 = \frac{1}{360}\psi^2X\Big(60A(3R^2 - X^2 - 3X - 3) + \psi^2\big(48R^5 - 90R^4 - 15R^2(X^3 + 2X^2 - 4) + 2(X^5 + 6X^4 + 15X^3 + 15X^2 - 9)\big)\Big). \tag{75}$$

By substituting the values of θ_0, θ_1 and θ_2 in the Eq. 9, the dimensionless temperature distribution of θ is obtained as follows:

$$\theta = 1 - \frac{1}{6}(A-1)\psi^2X\big(3 - 3R^2 + X(3+X)\big) + \frac{1}{360}\psi^4X(48R^5 - 90R^4 - 15R^2(X^2(X+2) - 4) + 2\big(3 + X(3+X)\big)\big(-3 + X(3+X)\big)\big)). \tag{76}$$

Calculation of thermal stresses in annular fin with hyperbolic profile

Assuming plane stress ($\sigma_z = 0$), radial and tangential stresses in axially symmetric state are defined as follows [18]:

$$\sigma_r = \frac{E}{1-\upsilon^2}\left[\left(\frac{du_r}{dr} - \gamma T\right) + \upsilon\left(\frac{u_r}{r} - \gamma T\right)\right], \tag{77}$$

$$\sigma_\theta = \frac{E}{1-\upsilon^2}\left[\left(\frac{u_r}{r} - \gamma T\right) + \upsilon\left(\frac{du_r}{dr} - \gamma T\right)\right], \tag{78}$$

where υ is Poisson's ratio, γ is thermal expansion coefficient, and E is Finn's modulus of elasticity. According to the classical theory of elasticity, the equilibrium equation in the polar coordinate system for a profile with variable thickness is as follows:

$$\frac{d\sigma_r}{dr} + \frac{\sigma_r}{t}\frac{dt}{dr} + \frac{\sigma_r - \sigma_\theta}{r} = 0. \tag{79}$$

By substituting the Eqs. 77 and 78 in Eq. 79, the displacement balance equation is obtained as follows:

$$\frac{d^2u_r}{dr^2} + \frac{(1+n)}{r}\frac{du_r}{dr} + \frac{(\nu n - 1)u_r}{r^2} - (1+\nu)\gamma\left(\frac{dT}{dr} + \frac{T}{r}n\right) = 0. \tag{80}$$

For dimensionless equation 80, the following dimensionless parameters are considered:

$$\overline{\sigma_r} = \frac{\sigma_r}{E}, \overline{\sigma_\theta} = \frac{\sigma_\theta}{E}, x = \frac{r}{r_a}, \theta = \frac{T - T_a}{T_b - T_a}, \chi = \gamma(T_b - T_a). \tag{81}$$

Considering the dimensionless parameters (Eq. 81), the following dimensionless temperature distribution equation is obtained as follows:

$$\frac{d^2u_r}{dx^2} + \frac{(1+n)}{x}\frac{du_r}{dx} + \frac{(vn-1)u_r}{x^2} - (1+v)r_a\chi\left(\frac{d\theta}{dx} + \frac{\theta}{x}n\right) = 0. \tag{82}$$

Also, the dimensionless form of stress equations (Eqs. 77 and 78) is obtained as follows:

$$\overline{\sigma_r} = \frac{1}{1-v^2}\left[\left(\frac{du_r}{dx} + v\frac{u_r}{x}\right)\frac{1}{r_a} - \chi(1+v)\theta\right], \tag{83}$$

$$\overline{\sigma_\theta} = \frac{1}{1-v^2}\left[\left(\frac{u_r}{x} + v\frac{du_r}{dx}\right)\frac{1}{r_a} - \chi(1+v)\theta\right], \tag{84}$$

and the boundary conditions without tension on the internal and external surfaces are as follows:

$$\overline{\sigma_r} = 0, \quad x = 1, R. \tag{85}$$

By changing the variable $X = x - 1$, the dimensionless temperature distribution (Eq. 76) is rewritten as follows:

$$\theta = 1 - \frac{1}{6}(A-1)\psi^2(x-1)(x^2 - 3R^2 + x + 1) + \frac{1}{360}\psi^4(48R^5(x-1) - 90R^4(x-1) + 8 + 2x^3(x^3-5) - 15R^2(x^4 - 2x^3 - 2x + 3). \tag{86}$$

By substituting the dimensionless temperature distribution (Eq. 86) in the differential equation 82 and solving this equation, the value of u_r is obtained.

Results of calculating the thermal stress of the annular fin with hyperbolic profile

In this section, HPM is first used to find the dimensionless temperature distribution of an isotropic annular fin with a hyperbolic profile and a variable thermal conductivity coefficient, and then the approximate analytical solution of the temperature distribution is used to calculate the thermal stresses. If $n = 0$ is substituted in Eq. 55, the fin will be annular with uniform thickness (rectangular profile) and therefore relations 82 and 41 will be the same. The results related to the annular fin with rectangular profile $(n = 0)$ are validated in section 6.

In the Figure 13, the effect of the thermal conductivity parameter (A) on the dimensionless temperature distribution is shown. As can be seen in this figure, the temperature decreases gradually from the base to the tip of the fin for different values of $A = -0.1, 0, 0.1$. Also, with the increase of A parameter, the dimensionless temperature increases and the local temperature drop is less.

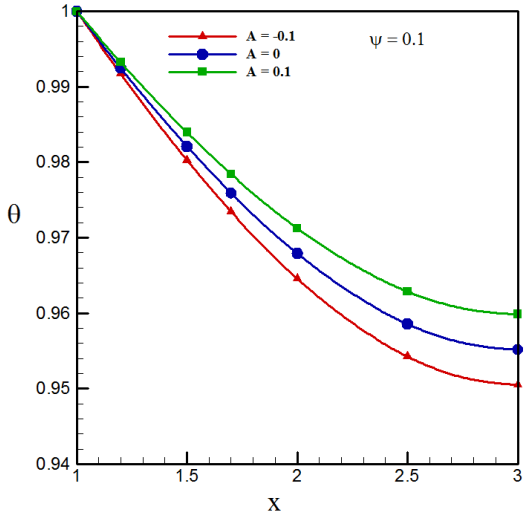

Figure 13. Effect of A on dimensionless temperature distribution.

In Figure 14, the temperature distribution changes for different values of ψ are shown. As can be seen, the temperature decreases from the base to the tip of the fin for $\psi = 0.1, 0.2, 0.3$ values. Also, with the increase of the ψ, the dimensionless temperature decreases and the local temperature drop is greater.

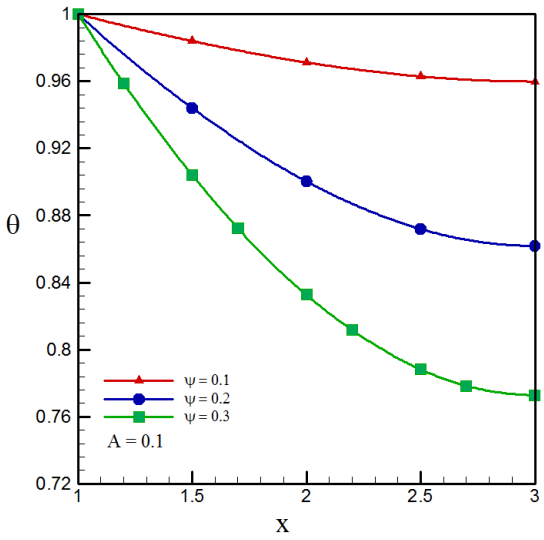

Figure 14. Effect of ψ on dimensionless temperature distribution.

In Figures 15 and 16, the effect of thermal conductivity parameter (A) on radial stress $\overline{\sigma_r}$ and tangential stress $\overline{\sigma_\theta}$ is shown. In these figures, the values of $\nu = 0.3$, $\psi = 0.1$ and $\chi = 1$ are considered. By examining these Figures, the radial stresses appear to be compressive while the tangential stresses are compressive near the base and tensile near the tip of the fin. It can also be seen that the absolute value of the stress increases with the decrease of the A.

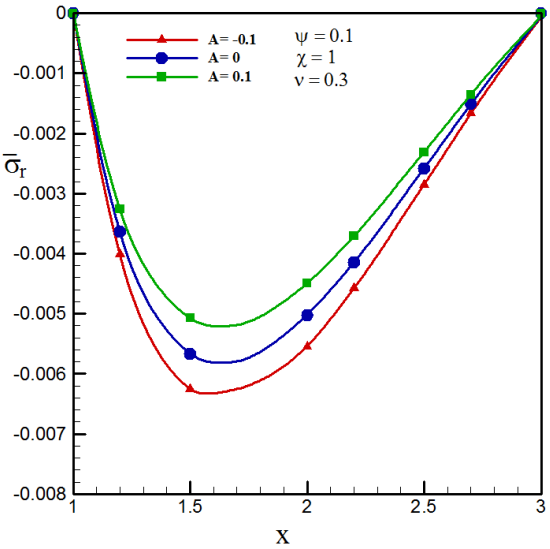

Figure 15. Effect of A parameter on radial stress.

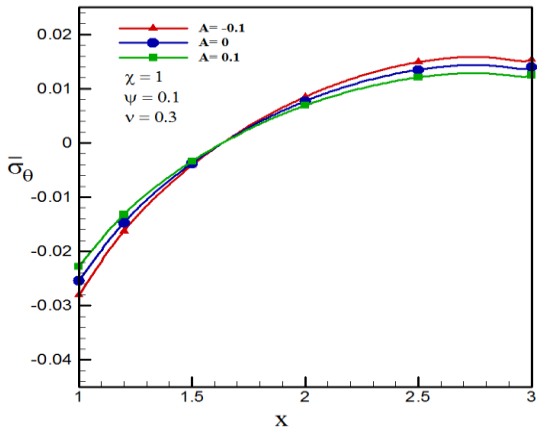

Figure 16. Effect of parameter A on tangential stress.

Figures 17 and 18 show the behavior of thermal stresses for $\psi = 0.1, 0.2, 0.3$. As can be seen, the radial stresses are compressive while the tangential stresses are compressive near the base and tensile near the tip of the fin. It can also be seen that the absolute value of the stress increases with the increase of the ψ.

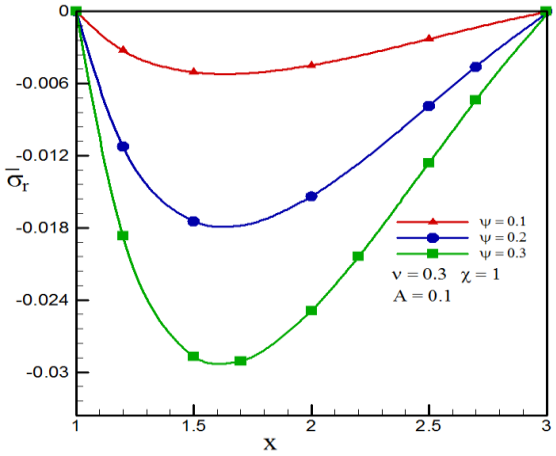

Figure 17. Effect of parameter ψ on radial stress.

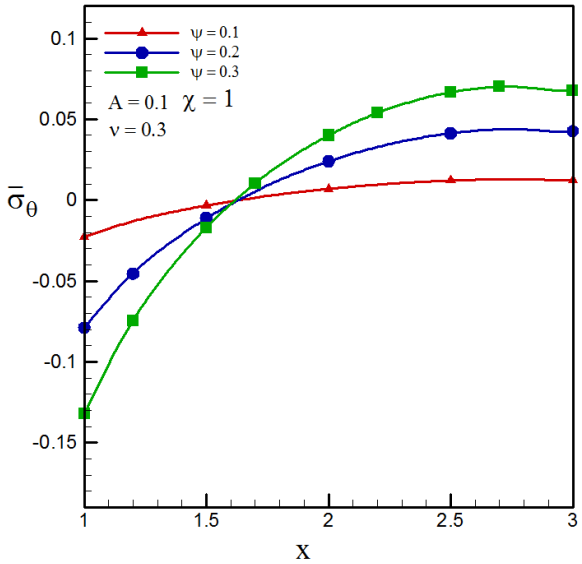

Figure 18. Effect of parameter ψ on tangential stress.

Figures 19 and 20 show the effect of thermal expansion parameter (χ) on radial and tangential stresses. As can be seen, the radial stresses appear to be compressive while the tangential stresses are compressive near the base and tensile near the tip of the fin. Also, with the increase of X, the absolute value of the stress increases.

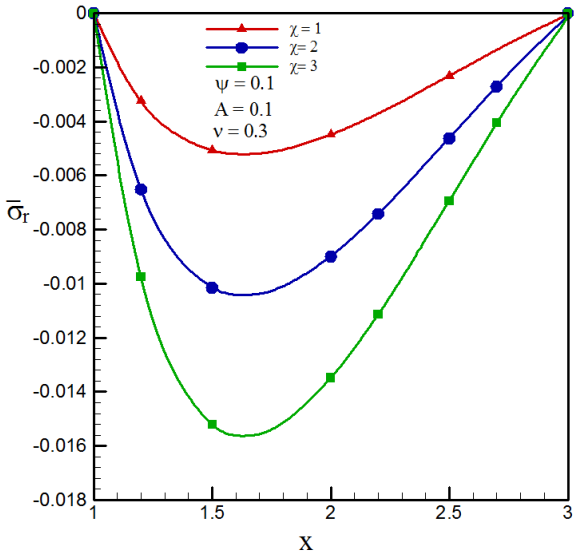

Figure 19. Effect of parameter χ on radial stress.

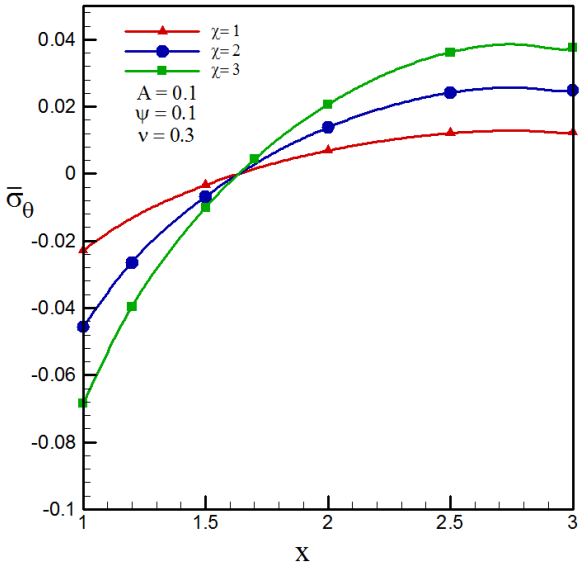

Figure 20. Effect of parameter χ on tangential stress.

Figures 21 and 22 show the effect of Poisson's ratio (υ) on radial and tangential stresses. As can be seen, the change of υ has a negligible effect on the radial and tangential stresses.

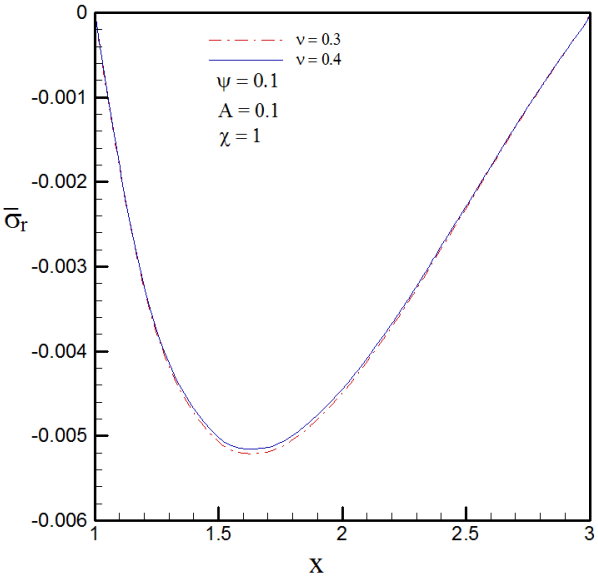

Figure 21. Effect of parameter υ on radial stress.

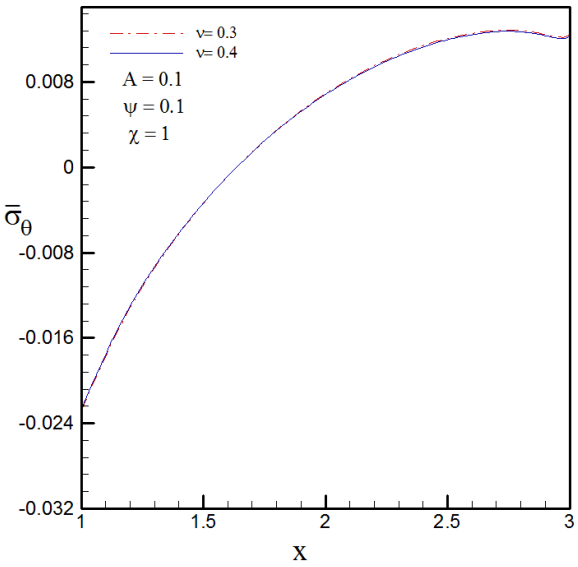

Figure 22. Effect of parameter υ on tangential stress.

By checking the Figures 13-22, it can be seen that the thermal stresses under the influence of the parameters A, ψ, χ and υ, while the temperature distribution is only affected by A and ψ. The highest absolute value of radial stress occurs at $x = 1.64$, the highest absolute value of tangential stress occurs at $x = 1$ (Fin base) and zero tangential stress value occurs at $x = 1.6352$. It can also be seen that the maximum value of the tangential stress is greater than the maximum value of the radial stress, so the most effective stress on fin failure is the tangential stress at the base of the fin.

Comparison of thermal stress of annular fins with rectangular and hyperbolic profile

In Figures 23 and 24, the radial and tangential stresses between the annular fin with rectangular profile $(n = 0)$ and the fin with hyperbolic profile $(n = -1)$ has been compared. As can be seen, the maximum value of the radial stress and tangential stress (at the base) in the fin with hyperbolic profile is less than the fin with rectangular profile. In fact, by changing the shape of the fin from rectangular (uniform thickness) to hyperbolic, the maximum value of radial and tangential stress decreases. These results show that due to the lower stress level of fin with

hyperbolic profile, it is much safer than fin with rectangular profile in terms of material failure. On the other hand, a fin with a hyperbolic profile is much more compact and requires less material to produce.

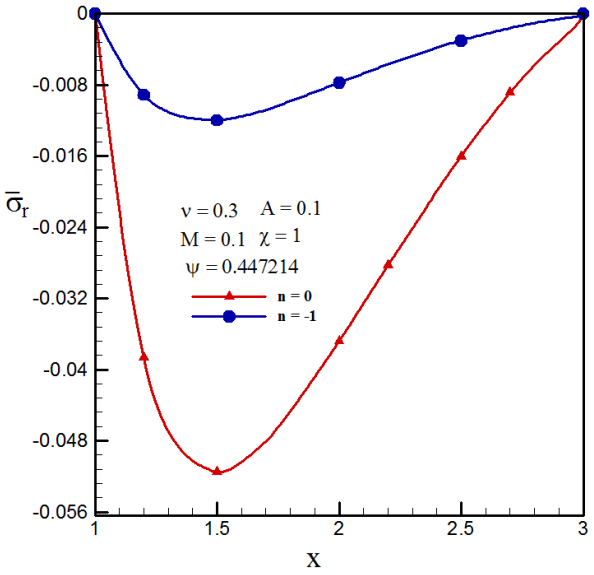

Figure 23. Comparison of radial stress between annular fins with rectangular and hyperbolic profiles.

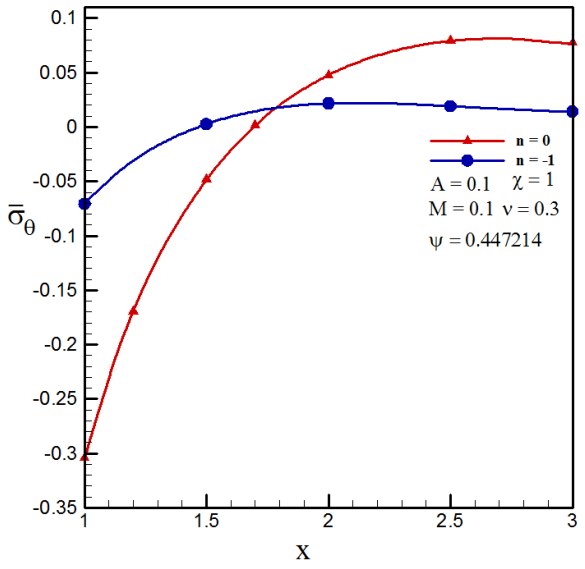

Figure 24. Comparison of tangential stress between annular fins with rectangular and hyperbolic profiles.

III. CONCLUSION

In this research, using HPM, the effect of thermal conductivity parameter (A), thermo-geometric parameter (M and ψ) and thermal expansion coefficient (χ) on the dimensionless temperature and thermal stresses of radiative-convective annular fin with rectangular profile and radiative-convective annular fin with hyperbolic profile with temperature-dependent thermal conductivity were calculated and compared. The main results of the present research are as follows:

- The homotopy perturbation method as a powerful tool is capable of solving nonlinear equations such as the energy equation related to the heat transfer of fins with appropriate accuracy and speed;
- The results of HPM are in good agreement with the analytical results or the results of other semi-analytical methods such as ADM and FDM;

- In annular fin with rectangular profile and annular fin with hyperbolic profile, the absolute value of stress increases with the decrease of thermal conductivity parameter;
- By increasing the parameter M in the annular fin with a rectangular profile, the absolute value of the stress increases, and by increasing the parameter ψ in the annular fin with a hyperbolic profile, the absolute value of the stress increases;
- By increasing the parameter χ in annular fins with rectangular and hyperbolic profiles, the absolute value of the stress increases;
- The parameter υ has no effect on the thermal stresses in the annular fin with a rectangular profile, and the parameter υ has a negligible effect on the thermal stresses in the annular fin with a hyperbolic profile;
- The maximum value of tangential stress is higher than the maximum value of radial stress. Therefore, the most effective stress on fin failure is the tangential stress at the base of the fin;
- By changing the shape of the fin from rectangular to hyperbolic, the maximum absolute value of radial and tangential stress decreases;
- A fin with a hyperbolic profile is much safer than a fin with a rectangular profile in terms of material failure due to the lower stress level. Also, fin with hyperbolic profile is much more compact and requires less materials for production.

As the development of the current research, the following will be considered in future works:

- Solving the nonlinear equation of convective radiative heat transfer in two-dimensional fins with constant cross-sectional area by HPM;
- Calculation of thermal stresses of annular fins with radiation and convection heat transfer by HPM.

IV. REFERENCES

[1] J.H. He, Homotopy perturbation technique, Computer Methods in Applied Mechanics and Engineering, 178 (3) (1999) 257-262.

[2] J.H. He, A coupling method of a homotopy technique and a perturbation technique for non-linear problems, International Journal of Non-Linear Mechanics, 35 (1) (2000) 37-43.

[3] C. Chiu, C. Chen, Thermal stresses in annular fins with temperature-dependent conductivity under periodic boundary condition, Journal of Thermal Stresses, 25 (5) (2002) 475-492.

[4] D.D. Ganji, Z.Z. Ganji, H.D. Ganji, Determination of temperature distribution for annular fins with temperature-dependent thermal conductivity by HPM, Thermal Science, 15 (1) (2011) 111-115.

[5] P.K. Roy, A. Mallick, Thermal analysis of straight rectangular fin using homotopy perturbation method, Alexandria Engineering Journal. 55 (3) (2016) 2269-2277.

[6] A. Mallick, R. Ranjan, P.K. Sarkar, Effect of heat transfer on thermal Stresses in an annular hyperbolic fin: an approximate analytical solution, Journal of Theoretical and Applied Mechanics, 54 (2) (2016) 437-448.

[7] R. Roy, S. Ghosal, Homotopy perturbation method for the analysis of heat transfer in an annular fin with temperature-dependent thermal conductivity, Journal of Heat Transfer, 139 (2) (2017) 022001-022008.

[8] G. Oguntala, G. Sobamowo, Y. Ahmed, R. Abd-Alhameed, Application of approximate analytical technique using the homotopy perturbation method to study the inclination effect on the thermal behavior of porous fin heat sink, Mathematical and Computational Applications. 23 (4) (2018) 62.

[9] T. Majhi, B. Kundu, New approach for determining fin performances of an annular disc fin with internal heat generation, Advances in Mechanical Engineering, Lecture Notes in Mechanical Engineering (2020) 1033-1043.

[10] O. Yontar, K. Aydin, I. Keles, Peractical jointed approach to thermal performance of functionally graded material annular fin, Journal of Thermophysics and Heat Transfer, 34 (1) (2020) 144-149.

[11] A. Irandegani, M. Sanjaranipour, F. Sarhaddi, Thermal performance evaluation of longitudinal fins with various profiles using homotopy perturbation method, Iranian Journal of Science and Technology, Transactions A: Science, 44 (6) (2020) 1761-1774.

[12] J.H. He, Y.O. El-Dib, Homotopy perturbation method with three expansions**,** Journal of Mathematical Chemistry, 59 (4) (2021) 1139-1150.

[13] J.H. He, Y.O. El-Dib, A.A. Mady, Homotopy perturbation method for the fractal toda oscillator**,** Fractal and Fractional, 5 (3) (2021) 93.

[14] G. Sowmya, R.S. Varun Kumar, M.D. Alsulami, B.C. Prasannakumara, Thermal stress and temperature distribution of an annular fin with variable temperature-dependent thermal properties and magnetic field using DTM-Pade approximant, Waves in Random and Complex Media, (2022) 1-29.
[15] M. Fallah Najafabadi, H. Talebi Rostami, D. Domiri Ganji, Temperature and Motion Analysis of a Rotational Maxwell Fluid with non-Constant Thermal Conductivity and non-Fourier Heat Transfer Model, International Journal of Applied and Computational Mathematics, 9 (1) (2023) 2.
[16] A. Irandegani, M. Sanjaranipour, F. Sarhaddi, Application of homotopy perturbation method to analyzing thermal behavior of moving longitudinal fins with various profiles, International Journal of Applied and Computational Mathematics, 10 (3) (2024) 119.
[17] C. Arsalanturk, Correlation equations for optimum design of annular fins with temperature dependent thermal conductivity, Heat and Mass Transfer, 45 (4) (2009) 519-525.
[18] S.P. Timoshenko, J.N. Goodier, Theory of Elasticity, McGraw-Hill, New York, 1970.
[19] A.P. Boresi, K.P. Chong, J.D. Lee, Elasticity in Engineering Mechanics, John Wiley and Sons, New Jersey, 2010.
[20] E.M.A. Mokheimer, Performance of annular fins with different profiles subject to variable heat transfer coefficient, International Journal of Heat and Mass Transfer, 45 (17) (2002) 3631-3642.